LA-2118

C.3

LOS ALAMOS SCIENTIFIC LABORATORY
OF THE UNIVERSITY OF CALIFORNIA o LOS ALAMOS NEW MEXICO

DELAYED NEUTRONS FROM FISSIONABLE ISOTOPES OF URANIUM, PLUTONIUM, AND THORIUM

LEGAL NOTICE

LA-2118
PHYSICS AND MATHEMATICS
(TID-4500, 13th edition)

LOS ALAMOS SCIENTIFIC LABORATORY
OF THE UNIVERSITY OF CALIFORNIA LOS ALAMOS NEW MEXICO

REPORT WRITTEN: February 1957

REPORT DISTRIBUTED: July 23, 1957

DELAYED NEUTRONS FROM FISSIONABLE ISOTOPES OF URANIUM, PLUTONIUM, AND THORIUM

by

G. R. Keepin
T. F. Wimett
R. K. Zeigler

Contract W-7405-ENG. 36 with the U. S. Atomic Energy Commission

ABSTRACT

The periods, relative abundances, and absolute yields of delayed neutrons from "fast" fission of six nuclides (U^{235}, U^{233}, U^{238}, Pu^{239}, Pu^{240}, and Th^{232}) and thermal fission of three nuclides (U^{235}, U^{233}, and Pu^{239}) have been measured. "Godiva," the bare U^{235} metal assembly at Los Alamos, was the neutron source. Six exponential periods were found necessary and sufficient for optimum least-squares fit to the data. Despite evident perturbations, general agreement among delayed neutron periods was obtained for all nuclides. Measured absolute total yields in delayed neutrons per fission (for the pure isotope) are:

U^{235}:	0.0165 ± 0.0005	Pu^{239}:	0.0063 ± 0.0003
U^{233}:	0.0070 ± 0.0004	Pu^{240}:	0.0088 ± 0.0006
U^{238}:	0.0412 ± 0.0017	Th^{232}:	0.0496 ± 0.0020

Representative of general delayed neutron periods (halflives) and abundances are the U^{235} fast-fission data:

Halflife (sec)	Relative Abundance
54.51 ± 0.94	0.038 ± 0.003
21.84 ± 0.54	0.213 ± 0.005
6.00 ± 0.17	0.188 ± 0.016
2.23 ± 0.06	0.407 ± 0.007
0.496 ± 0.029	0.128 ± 0.008
0.179 ± 0.017	0.026 ± 0.003

These data have been corroborated in detail by independent period-vs-reactivity measurements on the Godiva assembly. Period and abundance values for the various nuclides are compared and several mechanisms for perturbation of measured delayed neutron parameters are discussed.

ACKNOWLEDGMENTS

Gratitude is expressed to D. M. Barton, J. A. Grundl, B. A. Lindsey, E. A. Plassmann, A. A. Usner, and D. P. Wood of Group N-2, LASL, for assistance in taking the data; to J. V. Hamann, D. C. Hoffman, G. W. Knobeloch, E. J. Lang, F. Lawrence, and C. J. Orth of Group J-11, LASL, for the radiochemical determinations; and to Paul Harper and Roger Moore of Group T-1, LASL, for programming the general exponential decay problem.

CONTENTS

	Page
Abstract	3
Acknowledgments	5
I. Introduction	9
II. Experimental Arrangement and Measurement Techniques	12
III. Analysis of Delayed Neutron Data	22
IV. Experimental Results	29
A. Group Periods and Relative Abundance Values	29
B. Absolute Delayed Neutron Yields	31
V. Discussion of Results	39
Appendix. Sample Self-Multiplication Correction	51
References	53

I. INTRODUCTION

The first evidence for emission of neutrons following the fission process was reported by Roberts et al[1] shortly after the discovery of nuclear fission in 1939. These "delayed" neutrons, of reported halflife 12.5 ± 3 sec, were believed either to be photoneutrons produced by γ-activity of the fission fragments or to be emitted directly from one of the fission products. Subsequent yield measurements[2] quickly ruled out the first possibility; two months later the Bohr-Wheeler liquid-drop nuclear model was advanced,[3] thus providing a plausible mechanism for the experimental fact of delayed neutron emission.

Since the original work of Roberts, many investigations have been made on the characteristics of delayed neutrons; both accelerators and reactors have been used as neutron sources, with main interest in U^{235} and Pu^{239} thermal fission. For a résumé of previous investigations, reference is made to a recent review[4] summarizing all delayed neutron work prior to 1956. Comprehensive tables are included (for U^{235}, U^{233}, U^{238}, Pu^{239}, and Th^{232}) which compare directly the

reported work on the "well established" delayed neutron groups, i.e., those exhibiting periods between ~0.1 sec and ~1 min. Also reviewed are: (1) investigations of possible ultra-low-yield delayed neutron groups (very short or very long periods); (2) spectra and mean energies of delayed neutron groups (see also Batchelor and Hyder[5]); and (3) chemical identification of the delayed neutron precursors.

In general, the knowledge of delayed neutrons prior to the present investigation was completely satisfactory for most practical applications; e.g., measured periods, abundances, and total yields (for thermal fission) were quite adequate for calculating the kinetics of slow and intermediate systems with small available excess reactivity. In recent years, however, there has been increasing interest in intermediate and fast reactors, for which data have been inadequate.* Also the identification of delayed neutron precursors and their origin from fission products assumes some practical importance in the

*The trend toward intermediate and fast systems (e.g., fast power-breeder reactors utilizing U^{238} and Th^{232}) has pointed up the need for more basic data -- both differential and integral measurements -- in fast spectra. Increasing numbers of fast critical assemblies are being used for this purpose. The transient characteristics of these fast assemblies and their power-producing successors will, of course, be sensitively dependent on the periods and absolute yields of the delayed neutrons from fast fission.

control of high-power reactors (nuclear propulsion units, characterized by very high power densities and temperatures upwards of 5000°F, are perhaps an extreme example). There is, of course, continuing theoretical interest in detailed delayed neutron phenomena as an aid to further understanding of the fission process.

Considerations of this kind, coupled with the availability of a unique facility for delayed neutron studies (especially for the short periods where most uncertainty exists), led to the decision in 1954 to undertake an extended delayed neutron program at Los Alamos.* The major interest has been in fast fission, where accurate data are most needed. However, an attempt has been made to make the present measurements comprehensive and reasonably definitive.

---

*A preliminary report on status of the program was presented at the Geneva Conference, August, 1955.[6]

II. EXPERIMENTAL ARRANGEMENT AND MEASUREMENT TECHNIQUES

The complex decay of delayed neutron activity is capable of most direct and accurate analysis when the irradiation time of the fissile material is (a) "instantaneous," i.e., short compared to the shortest delayed neutron period, or (b) "infinite," i.e., long compared to the longest delayed neutron period. To minimize neutron multiplication within the sample, only a small amount (a few grams) of fissile material should be irradiated; this, in turn, implies the use of extremely high-intensity irradiations to provide adequate counting statistics. The bare U^{235} metal assembly at Los Alamos -- "Godiva"[7] -- is well suited to these requirements. With this assembly appropriately modified, both "infinite" and "instantaneous" irradiations, each consisting of $\sim 10^{16}$ total fissions, are used to emphasize the longer- and shorter-period contributions, respectively.* In

*"Infinite" irradiations refer to delayed critical operation; "instantaneous" irradiations are super-prompt-critical radiation bursts of <1/4 msec duration. Characteristics of

addition, the instantaneous irradiations provide an independent method of determining absolute total yield of delayed neutrons from the different fissile elements (cf. Section IV-B).

Measurements have been made on the delayed neutrons from fast fission of six nuclides: U^{235}, U^{233}, U^{238}, Pu^{239}, Pu^{240}, and Th^{232}, and from thermal fission of three nuclides: U^{235}, U^{233}, and Pu^{239}. The Godiva central spectrum (for "fast" neutron irradiations) is a slightly degraded fission neutron spectrum;[8] the "thermal" neutron spectrum is obtained within an 8 in. cubic polyethylene block, cadmium shielded and mounted near Godiva. The cadmium ratio of this moderator geometry was measured by U^{235}-foil activation as ~75, thus assuring a high preponderance of thermal fissions.

A schematic diagram of the general experimental arrangement for fast neutron irradiations is shown in Fig. 1; the

---

these bursts are discussed in Section V. The initial delayed neutron activity is proportional to $a_i \lambda_i$ following an instantaneous irradiation, and proportional to a_i for an infinite irradiation (a_i and λ_i are the abundance and decay constant, respectively, of the i^{th} delayed neutron group). This effective weighting of initial activity by the factor λ_i for an instantaneous irradiation is clearly advantageous in studying the short-period delayed neutron groups.

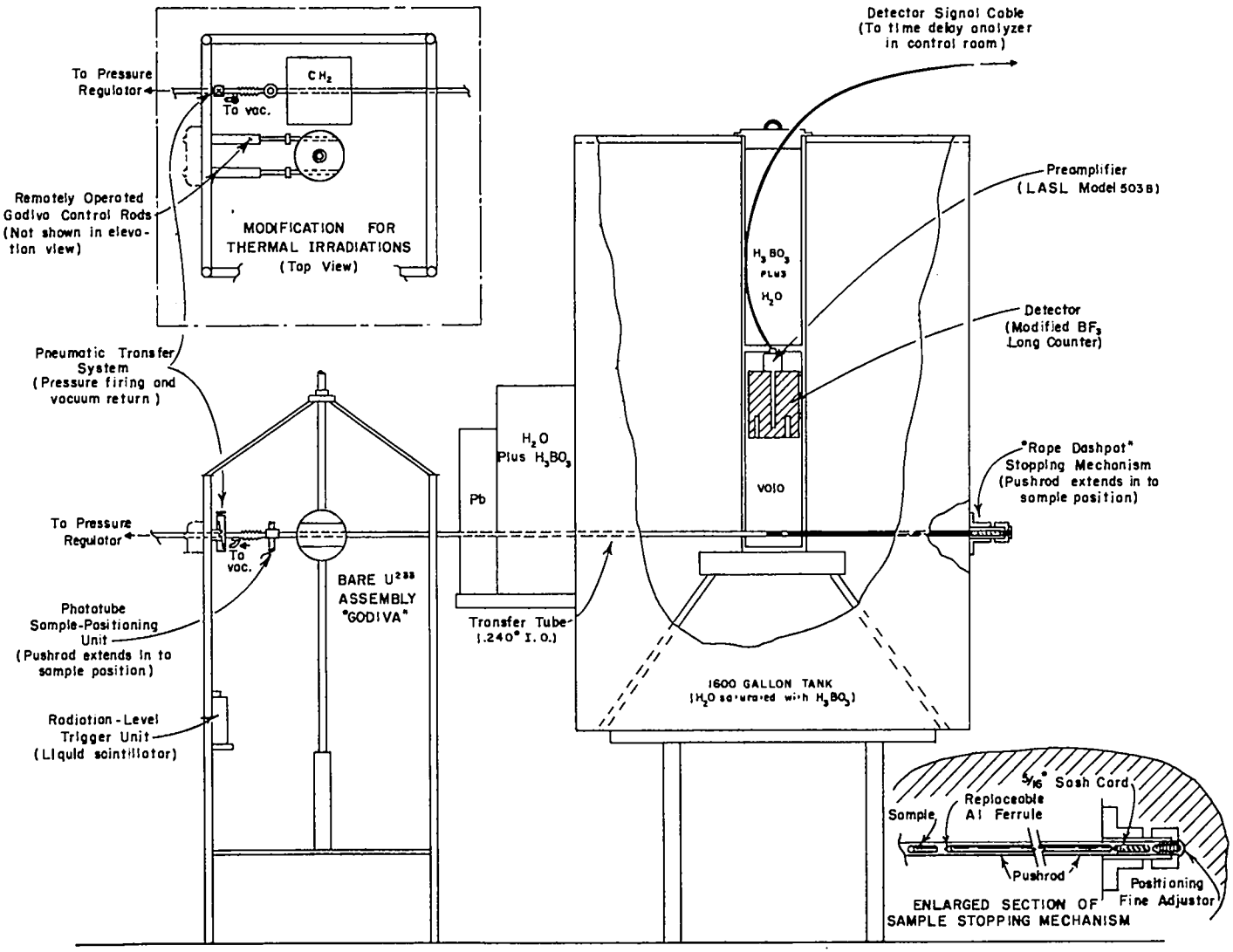

Fig. 1. Schematic diagram of the experimental arrangement for delayed neutron studies at Los Alamos.

modification for thermal neutron irradiations is indicated in the inset of Fig. 1. Photographs of the two arrangements are shown in Fig. 2. The Godiva assembly, sample transfer system, and detection equipment are located in an assembly building ("kiva") which is remotely operated from a control center 1/4 mile distant.[9]

A pneumatic system transfers a 2 to 5 g sample (~1/8 in. diameter) of fissile material from the point of irradiation to a 4π-shielded counting geometry in ~50 msec. Nickel-coated samples ($Pu^{239,240}$ and U^{233} with high specific α-activity) are protected from shock and abrasion by enclosure in thin titanium cans. Background measurements indicated no contribution from the titanium; this metal was also selected for its high strength-to-weight ratio. To minimize perturbation of the initial decay rate, it is required that the slug be stopped (without bouncing) reproducibly in the center of the counter geometry. A "rope dashpot" was found most effective for the purpose; this consists of a hollow steel pushrod (ideally of same mass as slug for complete momentum transfer) which impinges on a 6 in. length of 5/16 in. sash cord, the whole suitably enclosed in a steel cylinder. This transfer system was developed from a flexible test system using an improvised 1P41 phototube "bounce indicator" with pulse registration on a slow-sweep oscilloscope

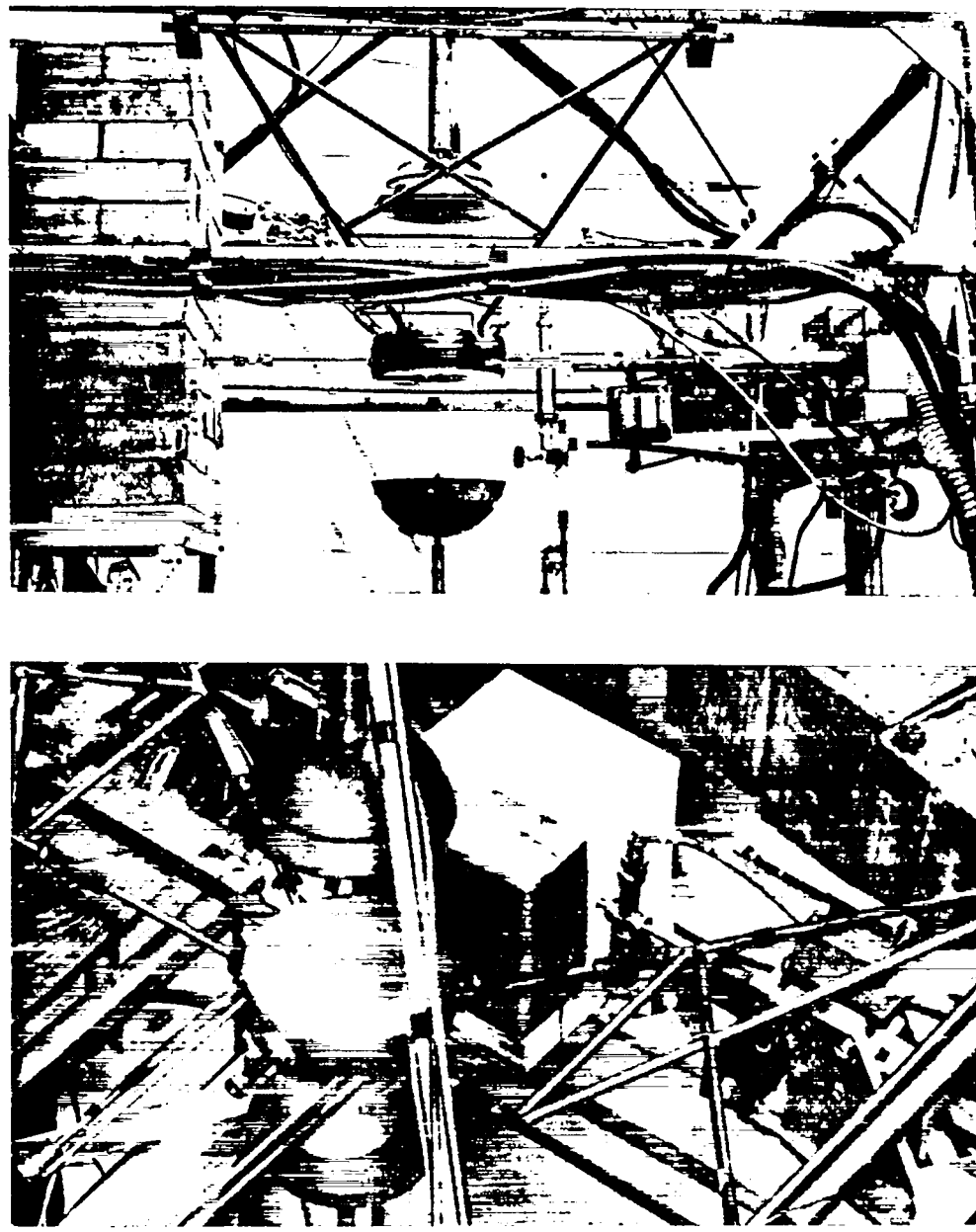

Fig. 2. The upper photograph shows the configuration for fast-fission irradiations with sample transfer tube through the central section and phototube positioning unit (small vertical shaft) on the right.
The lower photograph shows the modification for thermal irradiations; cf. schematic diagram, Fig. 1.

(Tektronix 512); "bounce" was ultimately reduced to less than 0.5 cm for 100 psi firing pressure.

A simple phototube arrangement ensures reproducible positioning of the sample within the center of Godiva (or polyethylene geometry) during irradiation. For instantaneous irradiations, the output of a scintillation detector is used to generate (at a preset radiation level) a "trigger" pulse which initiates sample transfer and counting. After the irradiated slug is counted for 500 sec, it is returned to Godiva by a remote-control vacuum system, thus completing an irradiation cycle.

The number of source fissions (relative "burst size") is determined by means of a gated U^{235} fission chamber which monitors the decay of Godiva neutron activity from 100 to 200 sec after the prompt burst.

The neutron detector used in the present work is a 1/2 in. diameter $B^{10}F_3$ proportional counter in "long" geometry, modified to give "flat" response within 5% from 23 kev to 1.5 Mev.* The essential modification from the original long-counter geometry of Hanson and McKibben[11] is the

---

*Some preliminary data were taken with a ZnS-boric acid scintillation detector[10] with neutron-to-gamma sensitivity ratio $>10^4$ and 1/v energy response. This was replaced by the BF_3 detector arrangement for improved ("flat") energy response and greater long-term stability.

addition of a shaped sleeve of boron plastic around the central BF_3 tube. The 5% error arises largely from uncertainty in calibration of the sources used: Sb-Be ($\bar{E}_n \sim$ 0.025 Mev), Po-Li ($\bar{E}_n \sim 0.4$ Mev), Po-LiF ($\bar{E}_n \sim 0.7$ Mev), and Mock Fission ($\bar{E}_n \sim 1.5$ Mev). Detector response was measured periodically with calibrated neutron sources and was found to be constant throughout the experiment. The BF_3 counter did not respond to gammas at the operating potential of 1200 v.

The counter signal was amplified by a LASL Model 503B preamplifier and Model 503 amplifier with auxiliary discriminator output. The dead time of the detection apparatus was determined to be 1 μsec. This was measured by plotting the ratio of detector counting rate to that of a desensitized BF_3 counter for various operating levels of Godiva. The slope of this curve was constant up to 5×10^4 counts/sec, yielding a dead time of 1 μsec.

The shielding for the counting geometry consists essentially of a cylindrical tank of water (6 ft in diameter and 9 ft high) saturated with boric acid. This was found to attenuate fission energy neutrons by a factor of $\sim 10^5$. Direct gamma shielding is provided by an 8-in.-thick lead shadow-shield between the reactor and detector, as shown in Fig. 1.

The decay of delayed neutron activity is monitored by a multichannel recording time-delay analyzer[12] with time-channel widths of 0.001, 0.01, 0.1, 1, and 10 sec following in automatic sequence; the number of channels of each width is variable, thus permitting selection of the most suitable channel-width distribution for a given decay curve. The analyzer (cf. Fig. 3) includes three basic units: (1) a four decade gated scaler with fast pulsed reset, (2) a 100 Kc crystal-controlled interval timer, and (3) a read-out coincidence circuit which duplicates the instantaneous reading of the gated scaler at intervals established by pulses from the timer unit. This duplicate reading is maintained for 0.5 msec, during which time it is permanently recorded either (1) photographically with a General Radio oscillograph camera or (2) electrically by direct print-out on Western Electric Teledeltos recording tape. Electrical print-out was used exclusively in the present work. The timer pulse automatically resets the gated scaler after each read-out, thus giving directly the differential number of counts per channel. This instrument was developed for studies (such as delayed neutron measurements) which encompass time scales from the millisecond region to the tens-of-seconds region; the time required to take equivalent data with a conventional time-delay analyzer would have been prohibitive.

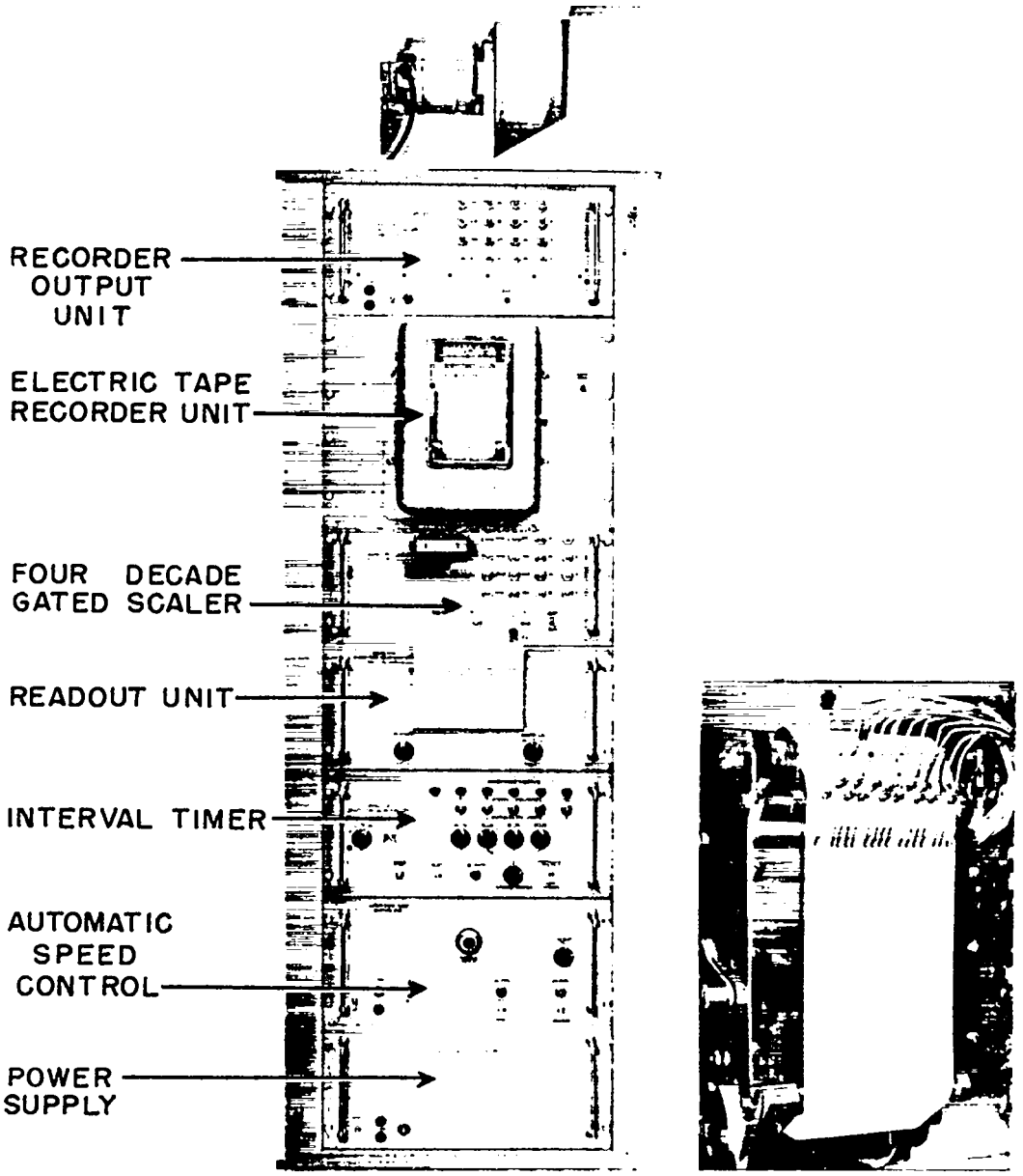

Fig. 3. Time-delay analyzer chassis with electrical printout. Inset at lower right shows recorder printing head in operation.

Two identical analyzers were built and operated in parallel, providing a continuous check on proper operation of the two independent systems. During each data run the two analyzers were checked for simultaneity of read-out. Following a run the two tapes were read and recorded; the readings of individual channels were required to agree to within one part in 10^4. It was further required that the sum of counts in all channels should agree with the number accumulated in a separate total-count scaler (LASL Model 800) which received the same signal input as the two analyzers. Accurate time-delay analysis was thus assured through independent checks on time-channel width, correct counts in each channel, and correct total counts.

Data are accumulated in groups of ten irradiations each which are corrected for counting loss (a few percent at most) and for background, if any. Corrected data are plotted and then punched onto IBM input data cards for least-squares analysis into periods and abundances as described in the following section.

III. ANALYSIS OF DELAYED NEUTRON DATA

It may be assumed that the decay of delayed neutron activity with time can be represented by a linear superposition of exponential decay periods. Thus if y represents the observed counting rate and t the independent variable time, we have

$$y = \sum_{j=1}^{k} A_j \; e^{-\lambda'_j t} \tag{1}$$

with the number of periods, k, to be determined. If a_{j_o}, λ_{j_o} are initial estimates of the "true" parameters, A_j and λ'_j, we then proceed by an iterative least-squares method to final values a_j, λ_j which minimize

$$\sum_{i=1}^{n} W_i \left(y_i - \sum_{j=1}^{k} a_j \; e^{-\lambda_j t} \right)^2 \tag{2}$$

where $W_i = 1/y_i$ is the weight associated with each observed y_i. To determine the optimum number of periods, preliminary analyses were made for k = 5, 6, and 7. Using five (or fewer)

periods, satisfactory convergence is not obtained and indicated errors are very large. When an arbitrary seventh period is introduced, the calculated abundance of this group is not significantly different from zero.* On the other hand, analyses using six delayed neutron groups have always led to rapid convergence with nominal errors on the final periods and abundances. Furthermore, six periods give the best least-squares fit, as indicated quantitatively by the "standard deviation of fit," a statistically defined figure-of-merit for curve fitting, described later in this section.

Two approaches to analysis of delayed neutron decay data have been investigated. The first is a simultaneous solution of all periods and abundances (12 x 12 matrix) from prompt-burst irradiation data. The second is a determination of the four long-period groups from long irradiation data and determination of the four shorter-period groups from burst irradiation data. The two sets of yields are then normalized at an appropriate point (in this case, at the second delayed neutron group). The latter method was found to give more accurate values of a_i and λ_i (smallest calculated errors) and has been used throughout the program. Thus, as expected, the more accurate computed values for

*Statistically a parameter is not significantly different from zero if the interval, parameter $\pm 2\sigma$, includes zero, where σ is the standard deviation of the parameter.

long periods are obtained from long irradiation data and similarly for the short periods from burst irradiation data.

For the long irradiation data, contributions from the two shortest periods clearly can be neglected for $t \geq 3.54$ sec.* Thus the data for $t \geq 3.54$ sec can be represented by

$$y = \sum_{j=1}^{4} A_j \, e^{-\lambda'_j t}$$

Let a_j, λ_j ($j = 1$ to 4) be estimates of A_j, λ'_j. Values of a_j, λ_j are obtained by finding values of these parameters which minimize the following expression

$$\sum_{i=1}^{n} W_i \left(y_i - \sum_{j=1}^{4} a_j \, e^{-\lambda_j t_i} \right)^2 \qquad (3)$$

where $W_i = 1/y_i$ is the weight associated with each observed y_i.

After the parameters a_j, λ_j are determined from the long irradiations, a correction is made to the burst irradiation data to account for contributions from the two long periods. Values of λ_1 and λ_2 obtained from the long irradiation data are used, and new values of a_1 and a_2 are

---

*$t = 3.54$ sec is a somewhat arbitrary "time-division" point. Independent checks have shown that final period and abundance values are insensitive to the exact choice of this time division point.

determined as follows

$$(a_1')_\infty = \frac{\sum_{i=80}^{500} y_i \text{ (from short irradiation)}}{\left(e^{-80\lambda_1} - e^{-500\lambda_1}\right) + R\left(e^{-80\lambda_2} - e^{-500\lambda_2}\right)}$$

where $R = 0.9502\ a_2/a_1$. The factor 0.9502 corrects for incomplete saturation of a_1 during a standard long irradiation. We have then

$$a_1' = (a_1')_\infty \lambda_1$$

$$(a_2')_\infty = R\ (a_1')_\infty$$

$$a_2' = (a_2')_\infty \lambda_2$$

For each y_i from the short irradiation, a corrected y_i' is determined from

$$y_i' = y_i - \left(a_1' e^{-\lambda_1 t_i} + a_2' e^{-\lambda_2 t_i}\right)$$

Using the y_i' values, parameters a_j, λ_j (j = 3 to 6) are obtained which minimize the expression

$$\sum_{i=1}^{n} W_i \left(y_i' - \sum_{j=3}^{6} a_j e^{-\lambda_j t_i}\right)^2 \qquad (4)$$

where $W_i = 1/y_i$.

To find the values of the parameters which minimize

Eqs. 3 and 4, the method of successive approximations is used. Let

$$y = \sum_{j=1}^{k} a_j \, e^{-\lambda_j t}$$

Approximate values a_{j_o}, λ_{j_o} are estimated for the parameters a_j and λ_j. In practice, these estimates are obtained from a preliminary graphical analysis of the delayed neutron decay curve. By expanding y in a Taylor's series about the approximations and discarding terms of second and higher order, we obtain

$$y \simeq \sum_{j=1}^{k} a_{j_o} \, e^{-\lambda_{j_o} t} + \sum_{j=1}^{k} \frac{\delta y}{\delta a_j} \Delta a_j + \sum_{j=1}^{k} \frac{\delta y}{\delta \lambda_j} \Delta \lambda_j \qquad (5)$$

where each partial derivative is evaluated at the point a_{j_o}, λ_{j_o} and where $\Delta a_j = (a_j - a_{j_o})$, $\Delta \lambda_j = (\lambda_j - \lambda_{j_o})$. Since Eq. 5 is a linear expression in Δa_j, $\Delta \lambda_j$, the usual methods for determining a weighted least-squares solution which minimizes

$$\sum_{i=1}^{n} W_i \left(y_i - \sum_{j=1}^{k} a_{j_o} \, e^{-\lambda_{j_o} t} - \sum_{j=1}^{k} \frac{\delta y}{\delta a_j} \Delta a_j - \sum_{j=1}^{k} \frac{\delta y}{\delta \lambda_j} \Delta \lambda_j \right)^2 \qquad (6)$$

can be applied. The resulting solutions for Δa_j, $\Delta \lambda_j$ are the corrections to be applied to the values a_{j_o}, λ_{j_o}. The

above procedure is then repeated with the corrected values as the starting point. Iteration is continued until convergence is obtained; i.e., the corrections Δa_j, $\Delta \lambda_j$ become very small ($\sim$1 part in 10^7) compared to the corresponding a_j and λ_j. That the final a_j and λ_j values are unique has been convincingly demonstrated by varying these values (as much as a few hundred percent) and then repeating the least-squares analysis. The iteration invariably converges on the unique ("best fit") values for a_j and λ_j.

Assuming y is normally distributed for each value of t, an estimate of the weighted variance of y is given by

$$s^2 = \frac{1}{n - k} \sum_{i=1}^{n} W_i \left(y_{obs} - y_{cal}\right)^2 \qquad (7)$$

where n is the number of data points, k is the number of parameters required in the least-squares fit, y_{obs} is the observed neutron decay data, and

$$y_{cal} = \sum_{j=1}^{k} a_j \, e^{-\lambda_j t}$$

The quantity s, given by Eq. 7, is the "weighted standard deviation of fit," the figure-of-merit for curve fitting referred to earlier. When the experiment is repeated, a different set of data is observed and different values of a_j, λ_j are obtained. Assuming that the distribution of these

parameters is normal, an estimate of their variances can be obtained. These are computed by finding the inverse of the matrix which occurs in the solution of the normal equations obtained from Eq. 6.[13] If the elements of the inverse matrix are denoted by C_{ij}, then estimates of the variance of individual a_j and λ_j parameters are given by

$$s^2_{a_1} = C_{11}\, s^2, \quad s^2_{a_2} = C_{22}\, s^2, \text{ etc.}$$

$$s^2_{\lambda_1} = C_{k+1,\, k+1}\, s^2, \quad s^2_{\lambda_2} = C_{k+2,\, k+2}\, s^2, \text{ etc.}$$

Thus, an estimate of the probable error associated with each parameter would be $0.6745\, s_{a_j}$, $0.6745\, s_{\lambda_j}$. Since the half-life is given by $\tau_{1/2} = \lambda^{-1} \ln 2$, an estimate of the standard deviation of $\tau_{1/2}$ is given by $s_{\tau_{1/2}} = \lambda^{-2}(\ln 2) s_\lambda$.

The general decay problem represented by Eq. 6 has been coded for the IBM 704 computer; this general code has proved very useful at LASL for several different problems requiring analysis of complex exponential decay curves. It is believed that the computer least-squares calculation completely eliminates subjective errors in decay curve analysis. Accepting the least-squares criterion for curve fitting, the computer gives unique period and abundance values which are by definition the "best fit" to a given set of experimental data.

IV. EXPERIMENTAL RESULTS

A. Group Periods and Relative Abundance Values

A summary of the results for high energy ("fast") fission is given in Table I. Relative abundance values include correction (<3%) for energy variation of the BF_3 detector response. These are prompt-burst irradiation results; as explained in Section III, values of τ_1, τ_2 and the abundance ratio a_1/a_2 are taken from final long irradiation data, and so are constant for each group. Final results (all data groups) for a given nuclide are obtained from a separate least-squares fit to all data -- not an average of individual data groups. The individual data groups (ten irradiations each) are tabulated to give the most direct presentation of experimental spread in the data. With a few exceptions (notably U^{238} and Th^{232} sixth group values) the observed experimental spread between corresponding group parameters for a given nuclide is seen to lie within calculated probable errors for these parameters. (Similar analysis in groups of ten irradiations each was performed on the long irradiations; the results are analogous to Table I and

TABLE I

FAST FISSION DELAYED NEUTRON DATA*

D.N. Group Index	HALFLIFE, $T_{1/2}$					RELATIVE ABUNDANCE, a_i/a					Absolute Group Yield (%) (for pure isotope)
	I	II	III	IV	All Data Groups	I	II	III	IV	All Data Groups	
"i"	U^{236} (89.9% 235; o/F = 0.0165 ± 0.0005)										
1	54.61 ±0.94	54.51 ±0.94	54.51 ±0.94	54.51 ±0.94	54.61 ±0.64	0.026±0.002	0.036±0.003	0.026±0.005	0.056±0.003	0.036±0.003	0.062±0.006
2	21.84 ±0.54	21.64 ±0.54	21.84 ±0.54	21.84 ±0.54	21.64 ±0.54	0.212±0.005	0.214±0.005	0.213±0.005	0.21±0.006	0.213±0.006	0.361±0.011
3	8.23 ±0.26	8.00 ±0.08	8.17 ±0.22	8.00 ±0.21	8.00 ±0.17	0.173±0.021	0.215±0.028	0.163±0.018	0.168±0.021	0.188±0.018	0.310±0.026
4	2.30 ±0.07	2.12 ±0.15	2.32 ±0.07	2.23 ±0.07	2.23 ±0.06	0.419±0.009	0.384±0.014	0.417±0.009	0.407±0.009	0.407±0.007	0.672±0.022
5	0.519±0.035	0.466±0.062	0.491±0.043	0.484±0.033	0.498±0.028	0.129±0.009	0.121±0.020	0.121±0.016	0.131±0.011	0.126±0.008	0.211±0.018
6	0.178±0.016	0.193±0.037	0.196±0.026	0.172±0.022	0.179±0.017	0.031±0.004	0.028±0.008	0.029±0.007	0.024±0.004	0.028±0.003	0.043±0.008
	U^{238} (99.98% 238; o/F = 0.0412 ± 0.0017)										
1	52.38 ±1.29	52.38 ±1.29	52.38 ±1.29	52.38 ±1.29	52.38 ±1.29	0.013±0.001	0.013±0.001	0.013±0.001	0.013±0.001	0.013±0.001	0.054±0.006
2	21.58 ±0.39	21.58 ±0.39	21.58 ±0.39	21.58 ±0.39	21.58 ±0.39	0.136±0.002	0.137±0.002	0.137±0.002	0.138±0.002	0.137±0.002	0.564±0.028
3	4.65 ±0.22	5.08 ±0.60	5.29 ±0.41	4.55 ±0.19	6.00 ±0.19	0.161±0.040	0.150±0.063	0.138±0.038	0.208±0.028	0.162±0.020	0.667±0.087
4	1.83 ±0.14	2.02 ±0.25	2.08 ±0.14	1.69 ±0.09	1.93 ±0.07	0.276±0.023	0.362±0.042	0.399±0.022	0.382±0.014	0.388±0.012	1.586±0.081
5	0.450±0.036	0.552±0.095	0.636±0.047	0.390±0.020	0.490±0.023	0.238±0.016	0.212±0.036	0.225±0.020	0.228±0.012	0.225±0.013	0.927±0.060
6	0.140±0.029	0.198±0.021	0.190±0.014	0.117±0.016	0.172±0.009	0.054±0.008	0.105±0.015	0.088±0.009	0.033±0.004	0.075±0.003	0.309±0.034
	U^{233} (100% 233; o/F = 0.0070 ± 0.0004)										
1	55.11 ±1.66	55.11 ±1.66	55.11 ±1.66	55.11 ±1.66	55.11 ±1.66	0.084±0.003	0.066±0.005	0.089±0.003	0.085±0.003	0.068±0.003	0.060±0.002
2	20.74 ±0.66	20.74 ±0.66	20.74 ±0.66	20.74 ±0.66	20.74 ±0.66	0.266±0.005	0.271±0.005	0.263±0.005	0.268±0.006	0.274±0.005	0.192±0.009
3	6.11 ±0.59	5.18 ±0.18	4.71 ±0.19	5.53 ±0.22	5.30 ±0.19	0.173±0.057	0.348±0.031	0.287±0.040	0.215±0.043	0.227±0.036	0.156±0.025
4	2.58 ±0.26	2.15 ±0.14	2.05 ±0.17	2.32 ±0.17	2.29 ±0.18	0.356±0.025	0.210±0.011	0.275±0.012	0.338±0.014	0.317±0.011	0.222±0.012
5	0.736±0.178	0.481±0.124	0.465±0.082	0.538±0.109	0.546±0.106	0.081±0.014	0.065±0.030	0.076±0.017	0.076±0.018	0.072±0.014	0.051±0.010
6	0.256±0.032	0.225±0.075	0.179±0.071	0.205±0.049	0.221±0.042	0.036±0.007	0.019±0.014	0.011±0.007	0.020±0.008	0.023±0.007	0.016±0.006
	Pu^{239} (99.8% 239; o/F = 0.0063 ± 0.0003)										
1	53.76 ±0.96	53.76 ±0.96	53.76 ±0.95	53.76 ±0.96	53.76 ±0.95	0.038±0.003	0.038±0.003	0.038±0.003	0.038±0.003	0.038±0.003	0.024±0.002
2	22.29 ±0.36	22.29 ±0.36	22.29 ±0.36	22.29 ±0.36	22.28 ±0.36	0.261±0.004	0.262±0.004	0.279±0.004	0.278±0.004	0.280±0.004	0.176±0.009
3	8.01 ±0.22	5.03 ±0.31	5.27 ±0.32	5.32 ±0.22	5.19 ±0.12	0.222±0.036	0.324±0.034	0.202±0.041	0.210±0.030	0.218±0.018	0.136±0.012
4	2.03 ±0.16	2.06 ±0.18	2.16 ±0.18	2.12 ±0.12	2.09 ±0.08	0.317±0.020	0.319±0.022	0.337±0.022	0.337±0.012	0.328±0.010	0.307±0.012
5	0.530±0.079	0.571±0.120	0.582±0.110	0.521±0.062	0.549±0.049	0.100±0.024	0.093±0.025	0.105±0.016	0.109±0.014	0.103±0.008	0.065±0.007
6	0.216±0.042	0.242±0.057	0.218±0.032	0.190±0.027	0.218±0.017	0.032±0.012	0.042±0.014	0.038±0.008	0.028±0.006	0.035±0.005	0.022±0.003
	Pu^{240} (81.5% 240; o/F = 0.0068 ± 0.0008)										
1	53.56 ±1.21	53.56 ±1.21	53.56 ±1.21	53.56 ±1.21	53.56 ±1.21	0.027±0.002	0.028±0.003	0.028±0.003	0.028±0.003	0.028±0.003	0.022±0.003
2	22.14 ±0.38	22.14 ±0.38	22.14 ±0.38	22.14 ±0.38	22.14 ±0.38	0.268±0.004	0.272±0.004	0.274±0.004	0.274±0.004	0.273±0.004	0.236±0.018
3	5.07 ±0.62	4.71 ±0.22	6.36 ±1.28	4.86 ±0.38	6.14 ±0.42	0.199±0.081	0.223±0.055	0.178±0.146	0.225±0.058	0.182±0.053	0.182±0.044
4	2.03 ±0.26	1.94 ±0.19	2.26 ±0.85	1.88 ±0.20	2.08 ±0.19	0.365±0.024	0.328±0.018	0.348±0.078	0.328±0.019	0.350±0.020	0.315±0.027
5	0.432±0.072	0.454±0.058	0.599±0.228	0.428±0.042	0.511±0.077	0.125±0.020	0.129±0.015	0.122±0.031	0.121±0.008	0.126±0.018	0.118±0.018
6	0.134±0.064	0.140±0.035	0.216±0.047	0.121±0.039	0.172±0.032	0.018±0.006	0.021±0.005	0.051±0.010	0.018±0.002	0.029±0.006	0.024±0.006
	Th^{232} (100% 232; o/F = 0.0496 ± 0.0020)										
1	56.03 ±0.95	56.03 ±0.95	56.03 ±0.95	56.03 ±0.95	56.03 ±0.96	0.034±0.002	0.034±0.002	0.034±0.002	0.033±0.002	0.034±0.002	0.186±0.012
2	20.76 ±0.66	20.76 ±0.66	20.75 ±0.66	20.75 ±0.66	20.75 ±0.66	0.151±0.005	0.151±0.005	0.150±0.005	0.148±0.005	0.150±0.006	0.744±0.037
3	4.96 ±0.24	8.60 ±0.33	5.66 ±0.41	6.62 ±0.87	5.74 ±0.24	0.208±0.033	0.156±0.031	0.162±0.035	0.115±0.037	0.156±0.021	0.788±0.108
4	1.92 ±0.11	2.16 ±0.12	2.05 ±0.10	2.50 ±0.20	2.16 ±0.06	0.417±0.031	0.429±0.022	0.465±0.018	0.428±0.047	0.446±0.018	2.212±0.110
5	0.502±0.057	0.576±0.066	0.461±0.028	0.671±0.132	0.571±0.042	0.159±0.019	0.172±0.022	0.174±0.007	0.177±0.018	0.172±0.013	0.853±0.073
6	0.182±0.032	0.223±0.030	0.105±0.024	0.212±0.128	0.211±0.019	0.031±0.008	0.045±0.010	0.015±0.002	0.101±0.010	0.043±0.008	0.213±0.031

*Notes: (a) Each data group (denoted by roman numerals) consists of 10 prompt burst irradiations with the exception of the U^{236} data which consist of 20 irradiations per group.

(b) Indicated for each nuclide are: 1) isotopic purity of sample used, and 2) o/F = total absolute yield in delayed neutrons per fission; note that o/F values (and absolute group yields) have been corrected to 100% isotopic purity; cf. Section IV-B.

(c) Uncertainties indicated are calculated probable errors (from IBM-704 computer).

(d) T_1,T_2 and the ratio a_1/a_2 are taken from final long irradiation data (cf. Section III).

(e) $\sum a_i = a = o/F$ = total delayed neutrons per fission. Abundance values reported include correction (< 2%) for energy variation of detector response.

are not included here.)

Thermal fission results are summarized in Table II. The analysis of these data is identical with that for fast fission.

Figure 4 shows the agreement between the experimental data for fast fission of U^{235} and a curve calculated from the periods and abundances reported for U^{235} in Table I. Agreement of this kind was obtained for the delayed neutron decay curve of each fissionable nuclide studied. During the course of the program, approximately 1000 irradiations were made on Godiva, with nearly equal numbers of prompt bursts and long irradiations.

B. Absolute Delayed Neutron Yields

Absolute delayed neutron yield may be measured using either prompt bursts or infinite (delayed critical) irradiations. The former is considerably more accurate since in this case yield is determined from neutron total counts following the burst, whereas yield can be determined only from initial (t = 0 extrapolation) neutron counting rate following a saturation irradiation.

The basic data for determining absolute yield by the prompt burst method are: (1) $\Sigma_{NC} \equiv$ total neutron counts (corrected for detector loss and background) following an instantaneous irradiation, (2) $\epsilon \equiv$ absolute efficiency of

TABLE II

THERMAL FISSION DELAYED NEUTRON DATA*

D.N. Group Index "i"	HALFLIVES, $T_{1/2}$					RELATIVE ABUNDANCE, a_i/a					Absolute Group Yield (%) (for pure isotope)
	I	II	III	IV	All Data Groups	I	II	III	IV	All Data Groups	
	U^{235} (99.9% 236; n/F = 0.0158 ± 0.0005)										
1	55.72 ±1.28	56.72 ±1.28	55.72 ±1.28	55.72 ±1.28	55.72 ±1.28	0.022±0.002	0.033±0.002	0.032±0.003	0.032±0.003	0.033±0.003	0.062±0.006
2	22.72 ±0.71	22.72 ±0.71	22.72 ±0.71	22.72 ±0.71	22.72 ±0.71	0.218±0.009	0.220±0.008	0.217±0.009	0.220±0.009	0.218±0.009	0.348±0.018
3	6.19 ±0.46	6.17 ±0.49	6.26 ±0.77	6.44 ±0.71	6.22 ±0.23	0.196±0.046	0.198±0.047	0.183±0.072	0.182±0.059	0.188±0.022	0.310±0.038
4	2.30 ±0.18	2.26 ±0.17	2.34 ±0.34	2.40 ±0.24	2.30 ±0.09	0.395±0.024	0.396±0.020	0.390±0.058	0.397±0.029	0.395±0.011	0.624±0.028
5	0.614±0.108	0.560±0.069	0.743±0.361	0.666±0.131	0.610±0.083	0.116±0.019	0.120±0.020	0.102±0.028	0.124±0.014	0.115±0.009	0.182±0.018
6	0.230±0.031	0.206±0.025	0.265±0.036	0.226±0.026	0.230±0.025	0.040±0.009	0.033±0.009	0.066±0.020	0.040±0.009	0.042±0.008	0.066±0.008
	Pu^{238} (99.8% 239; n/F = 0.0061 ± 0.0003)										
1	54.28 ±2.34	54.28 ±2.34	54.28 ±2.34	54.28 ±2.34	54.28 ±2.34	0.033±0.009	0.032±0.009	0.032±0.008	0.036±0.010	0.035±0.009	0.021±0.006
2	23.04 ±1.67	23.04 ±1.67	23.04 ±1.67	23.04 ±1.67	23.04 ±1.67	0.293±0.035	0.294±0.035	0.294±0.035	0.318±0.038	0.298±0.035	0.182±0.023
3	6.72 ±0.37	5.92 ±0.49	4.51 ±0.35	6.38 ±0.91	5.60 ±0.40	0.225±0.043	0.203±0.051	0.174±0.078	0.264±0.078	0.211±6.048	0.129±0.030
4	2.03 ±0.19	2.19 ±0.25	1.91 ±0.37	2.42 ±0.44	2.12 ±0.24	0.333±0.028	0.338±0.034	0.340±0.068	0.262±0.060	0.328±0.033	0.189±0.022
5	0.500±0.158	0.622±0.190	0.594±0.399	0.845±0.222	0.616±0.212	0.089±0.042	0.090±0.025	0.098±0.018	0.077±0.058	0.088±0.028	0.052±0.018
6	0.220±0.083	0.241±0.040	0.263±0.083	0.297±0.030	0.257±0.045	0.027±0.021	0.043±0.013	0.063±0.011	0.045±0.029	0.044±0.018	0.027±0.010
	U^{252} (100% 233; n/F = 0.0066 ± 0.0003)										
1	56.00 ±0.54	55.00 ±0.54	55.00 ±0.54	55.00 ±0.54	55.00 ±0.54	0.087±0.003	0.086±0.002	0.087±0.002	0.087±0.003	0.086±0.003	0.057±0.003
2	20.57 ±0.28	20.57 ±0.36	20.57 ±0.36	20.57 ±0.38	20.57 ±0.38	0.301±0.004	0.299±0.004	0.300±0.004	0.299±0.004	0.299±6.004	0.187±0.008
3	4.68 ±0.16	5.20 ±0.29	4.90 ±0.34	5.12 ±0.26	5.00 ±0.21	0.292±0.030	0.322±0.044	0.261±0.074	0.236±0.047	0.252±0.040	0.168±0.027
4	1.90 ±0.21	2.17 ±0.16	2.20 ±0.52	2.18 ±0.21	2.13 ±0.20	0.246±0.029	0.305±0.011	0.247±0.067	0.295±0.018	0.278±0.020	0.184±0.018
5	0.566±0.548	0.445±0.048	0.787±0.454	0.542±0.297	0.615±0.242	0.035±0.051	0.063±0.007	0.061±0.023	0.052±0.050	0.061±6.024	0.034±0.018
6	0.300±0.074	0.171±0.050	0.296±0.027	0.260±0.102	0.277±0.047	0.039±0.020	0.018±0.002	0.044±0.007	0.029±0.030	0.034±0.014	0.022±0.009

*Notes: (a) Each data group (denoted by roman numerals) consists of 10 prompt burst irradiations.

(b) Indicated for each nuclide are: (1) isotopic purity of sample used, and 2) n/F = total absolute yield in delayed neutrons per fission; note that n/F values (and absolute group yields) have been corrected to 100% isotopic purity; cf. Section IV-B.

(c) Uncertainties indicated are calculated probable errors (from IBM-704 computer).

(d) T_1, T_2 and the ratio a_1/a_2 are taken from final long irradiation data (cf. Section III).

(e) $\Sigma a_i = a = n/F$ = total delayed neutrons per fission. Abundance values reported include correction (< 3%) for energy correction of detector response.

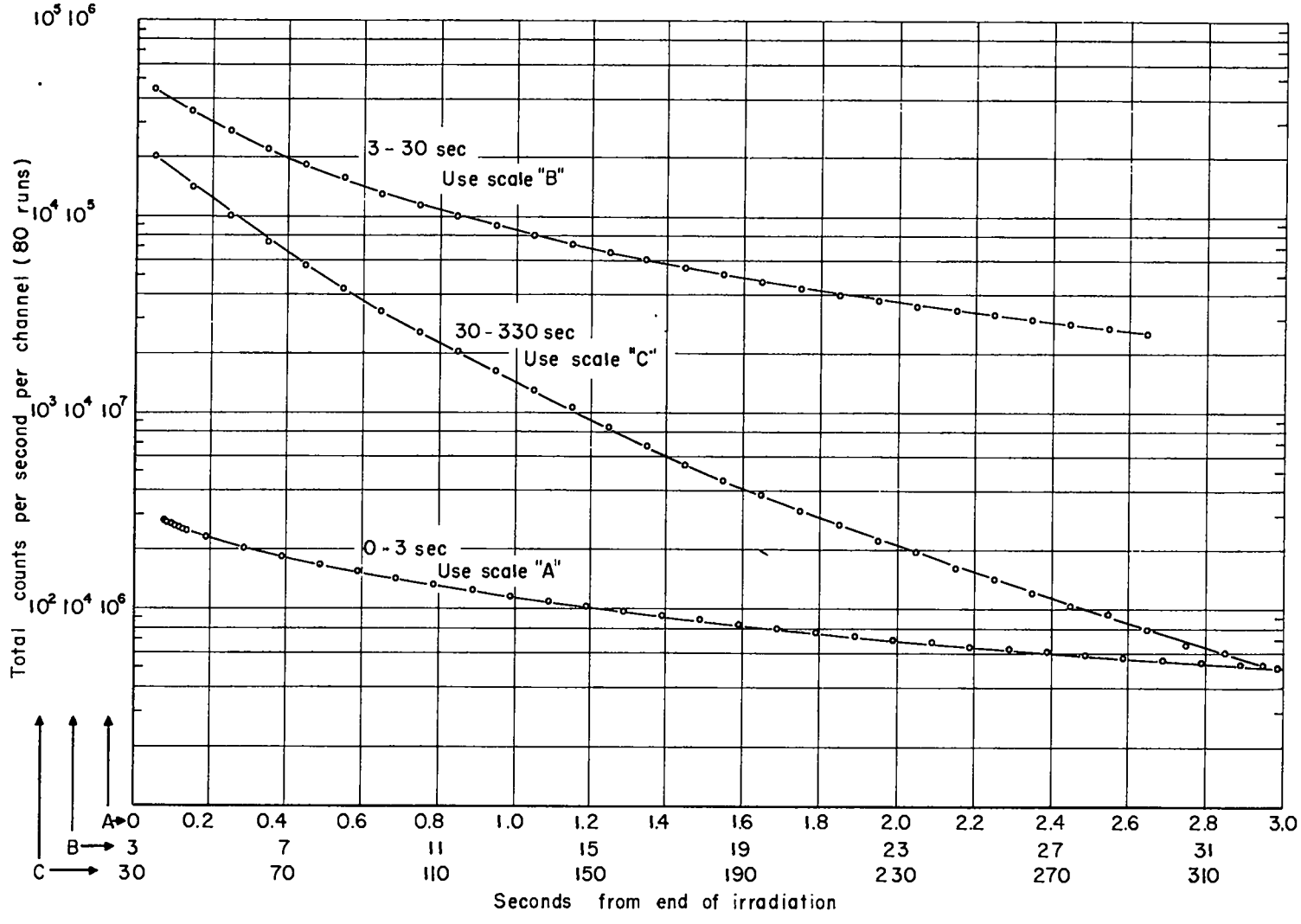

Fig. 4. Delayed neutron decay following instantaneous irradiations of U^{235} (fast fission). Cumulative data (o) from 80 prompt burst irradiations of 3 g sample of 99.9% U^{235}; the curve is calculated from the U^{235} periods and abundances of Table I.

the neutron detector, and (3) $F_s \equiv$ total fissions in the sample irradiated. In the present measurements total fissions are determined by standard counting of the 67 hr β-activity from Mo^{99}; i.e., all fission-produced Mo^{99} is chemically separated from the irradiated sample and a known aliquot is β-counted in standard geometry. Measured β-yield is then converted to number of fissions which occurred in the sample by an appropriate "K factor." K factors for the various fissionable materials are determined from a primary calibration of number of fissions in a thin fissile foil of known weight against Mo^{99} β-yield from a thick foil also of known weight; both foils are irradiated in the same neutron flux. K factors for the various nuclides studied have been redetermined recently,[14] and these best values (accurate to within 4%) have been used here. Absolute efficiency of the (flat-response) neutron detector is determined with calibrated neutron sources (cf. Section II). Thus for an instantaneous irradiation

$$\Sigma_{NC} = F_s \epsilon \sum_{i=1}^{6} \int_{o}^{\infty} a_i \lambda_i e^{-\lambda_i t} dt = F_s \epsilon \sum_{i=1}^{6} a_i \qquad (8)$$

where t is measured from the time of the burst

a_i = abundance of i^{th} group, in delayed neutrons per fission

λ_i = decay constant of i^{th} group

Σa_i = n/F $\equiv$ absolute yield in total delayed neutrons per fission

$\therefore$ absolute yield = (n/F) = $\Sigma_{NC}/F_s\epsilon$

Since the initial counting rate following an infinite irradiation is proportional to Σa_i (or n/F), this method may be used to check the more precise yield values as obtained above from the instantaneous irradiation data.

A small correction (order of 1%) must be applied to n/F values as obtained above due to the self-multiplication of the sample irradiated (cf. Appendix). Final values of absolute total yields, corrected to 100% isotopic purity, are presented in Table III.

Within the error of these measurements, no "spectral effect" (i.e., dependence on energy of neutrons inducing fission) was observed for the absolute yields of U^{235}, U^{233}, and Pu^{239}. The values given in Table III were tabulated in order of increasing yield to emphasize two interesting regularities: (1) total yield increases with mass number for a given element and (2) total yield generally decreases with atomic number [except in extreme cases where (1) predominates over (2), e.g., Pu^{240} vs U^{233}].

The delayed neutron fraction of total neutrons from fission, defined as β (or "f"), may be obtained from absolute

TABLE III

ABSOLUTE TOTAL YIELDS OF DELAYED NEUTRONS

Fissile Nuclide	Absolute Yield (Delayed Neutrons/Fission for Pure Isotope)	
	Fast Fission	Thermal Fission
Pu^{239}	0.0063 ± 0.0004[a] 0.0063 ± 0.0003[b]	0.0061 ± 0.0003[b] 0.0062 ± 0.0004[c]
	Final 0.0063 ± 0.0003	Final 0.0061 ± 0.0003
U^{233}	0.0072 ± 0.0004[a] 0.0068 ± 0.0004[b]	0.0067 ± 0.0004[b] 0.0065 ± 0.0003[c]
	Final 0.0070 ± 0.0004	Final 0.0066 ± 0.0003
Pu^{240}	Final 0.0088 ± 0.0006[b]	---
U^{235}	0.0163 ± 0.0007[a] 0.0166 ± 0.0007[b]	0.0157 ± 0.0007[b] 0.0159 ± 0.0007[c]
	Final 0.0165 ± 0.0005	Final 0.0158 ± 0.0005
U^{238}	0.0426 ± 0.0028[a] 0.0403 ± 0.0019[b]	---
	Final 0.0412 ± 0.0017	
Th^{232}	0.0499 ± 0.0030[b] 0.0493 ± 0.0030[c]	---
	Final 0.0496 ± 0.0020	

[a] Measurements of June 1955, originally reported at Geneva; values are corrected for a small systematic error which was eliminated in subsequent measurements. The large absolute yield for Th^{232} reported at Geneva was in error, due to incomplete recovery of tracer molybdenum. (Special techniques are required to ensure that thorium slugs are completely dissolved, prior to radiochemical analysis.)

[b] Measurements of November 1956 (weighted average).

[c] Measurements of January 1957 (weighted average).

"Final" values are weighted averages of all determinations; the indicated uncertainties are probable errors (to conform with calculated uncertainties on a_i and τ_i in Tables I and II).

total delayed neutron yield (n/F) by the relation $\beta = (n/F)\bar{\nu}^{-1}$, where $\bar{\nu}$ is the average number of neutrons emitted per fission. $\bar{\nu}$ values for thermal neutron fission are taken from Geneva average data.[15] $\bar{\nu}$ (E) values for fast fission were deduced mainly from the slopes, $d\bar{\nu}/dE_n$, given by Terrell[16] and by Leachman,[17] and then weighted by the appropriate fission cross section in the Godiva central flux spectrum to give the $\bar{\nu}$ values for fast fission. These values of $\bar{\nu}$ and the resulting values for β are presented in Table IV.

TABLE IV

$\bar{\nu}$ AND β VALUES FOR SIX FISSILE NUCLIDES*

Fissile Nuclide	Fast Fission ($\bar{E}_n$ ~ Fission Spectrum)	Thermal Fission
Pu^{239}	$\bar{\nu}$ = 3.01 ± 0.09 β = 0.0020_9 ± 0.0001_6	$\bar{\nu}$ = 2.91 ± 0.06 β = 0.0021_0 ± 0.0001_6
U^{233}	$\bar{\nu}$ = 2.63 ± 0.08 β = 0.0026_6 ± 0.0001_7	$\bar{\nu}$ = 2.55 ± 0.06 β = 0.0025_9 ± 0.0001_8
Pu^{240}	$\bar{\nu}$ = 3.42 ± 0.20 β = 0.0025_7 ± 0.0003_0	
U^{235}	$\bar{\nu}$ = 2.56 ± 0.06 β = 0.0064_5 ± 0.0003_3	$\bar{\nu}$ = 2.47 ± 0.05 β = 0.0064_0 ± 0.0003_2
U^{238}	$\bar{\nu}$ = 2.62 ± 0.13 β = 0.0157 ± 0.0012	
Th^{232}	$\bar{\nu}$ = ~2.3 β = ~0.022	

* $\bar{\nu}$ ≡ average number of neutrons emitted per fission; β ≡ delayed neutron fraction of total neutrons from fission. $\bar{\nu}$ values were obtained from data in Refs. 15, 16, and 17. β values are calculated from the absolute total yields given in Table III by the relation $\beta = (n/F)\bar{\nu}^{-1}$. Indicated uncertainties are standard deviations.

V. DISCUSSION OF RESULTS

In Tables I and II the individual group periods for the various fissile nuclides studied are seen to be in general agreement. As would be expected, smaller errors on a_i and τ_i are generally associated with larger group abundances. A comparison of individual delayed neutron groups among the various nuclides shows that (1) variation among group yields is much greater than variation among group periods, and (2) the increase of total yield with mass number is due mainly to greater contribution from the shorter-period groups.

General agreement will be noted among both periods and abundances for thermal fission in Table II and corresponding data for fast fission in Table I. For thermal irradiations, the characteristic burst width ($\sim$0.2 msec) is unavoidably lengthened by neutron diffusion time (fraction of a millisecond) in the polythene moderating geometry. In principle this would tend to lengthen the sixth delayed neutron period but not enough to be detectable. Small spectral differences (especially for fifth and sixth group values) could, of course, result from the variation in fission mass-distribution

with incident neutron energy. It will be recalled (cf. Table III) that no spectral effect was observed for absolute total delayed neutron yields.

It may be pointed out that better statistics were purposely obtained for the fast fission data and this is reflected in smaller errors on a_i and τ_i than were computed for the corresponding thermal fission data. Thus for practical applications, if one considers the delayed neutron periods and abundances for a given nuclide as essentially independent of neutron spectrum, it is recommended that the more accurate fast fission results be used.

The period and abundance values reported in Table I are in substantial agreement with preliminary data reported for fast fission at Geneva;[6] an exception is the sixth-group halflife. Present values of τ_6 for the fissile elements studied are seen to agree within calculated errors. The U^{238} burst irradiations provide the most accurate value of τ_6, 0.172 ± 0.009, which does agree with the preliminary (1955) value of 0.18 ± 0.02. This precision is possible in the case of U^{238} due to the exceptionally large abundance of the sixth group.

A comparison of U^{235} data with the earlier work of

Hughes et al.[18] has been made.* Notable differences (mainly in third- and fourth-group periods) were attributed largely to (1) different amounts of data in the appropriate time interval -- 5 to 40 sec and (2) the different methods of analysis -- least-squares fit vs the more subjective graphical "exponential peeling" method.

Despite the general agreement observed among group periods there do exist mechanisms whereby real differences can arise (I) between measured delayed neutron periods and their corresponding precursor β-decay periods and (II) between corresponding delayed neutron periods for the different fissile nuclides.

Delayed neutron precursors can be formed either directly as primary fission products or by cascade β-decay from primary fission products. In the latter case, precursor activity (and hence delayed neutron activity) would exhibit a growth-decay characteristic with time. The over-all effect of this "growth-decay" perturbation will be a lengthening of observed precursor period (cf. difference I above), the magnitude of the perturbation being dependent on the β-periods

---

*The periods measured by Hughes, Dabbs, Cahn, and Hall at Argonne are 55.6, 22.0, 4.51, 1.52, 0.43, and 0.05 sec; abundances are roughly comparable to those given for U^{235} in Tables I and II. The comparison referred to is made in Ref. 4, p. 200ff.

involved. A small effect clearly cannot be resolved in the analysis of neutron decay curves, and the perturbation will in effect be propagated cumulatively from the precursor directly involved to all subsequent (shorter) groups.

A possible consequence of the growth-decay effect could be a slight dependence of measured delayed neutron periods on the length of irradiation; i.e., a complex β-decay scheme "feeding" a delayed neutron precursor could result in different observed periods as the irradiation time is changed. In this connection it is interesting that third- and fourth-group period values determined from the long irradiations are somewhat smaller than the more precise values obtainable from prompt burst data.

The differences in corresponding delayed neutron periods for the six fissile nuclides (difference II above) arise basically from variations in independent nuclide yield. For a given nuclide this yield is determined by the appropriate yield-mass* and charge distributions. Both of these distributions are in turn dependent on the identity of the fissile nuclide and the energy of the neutrons inducing fission. It

---

*Here we consider relatively minor perturbations such as "post-fission neutron boil-off"[19] as an intrinsic property of the yield-mass distribution since the occurrence of fission and post-fission neutron emission are experimentally indistinguishable in time.

follows that differences in observed periods (and abundances) could be introduced by (a) changes in the growth-decay characteristics of a fission chain "feeding" a given precursor and/or (b) the small differential contributions of minor delayed neutron precursors (i.e., other than the six main group precursors).

Theoretically there will be slight perturbations of delayed neutron periods and abundances due to self-multiplication of the sample. From reactor kinetic theory we know that the neutron decay periods observed following fission will approach asymptotically the "true" delayed neutron periods only in the limit of infinitely negative reactivity, i.e., for an infinitesimal sample. This effect will be quite negligible for the small samples used here -- a few grams at most. Secondly, there is a small spectral effect arising from different effectiveness of the various delayed neutron groups in producing fissions in the sample. This spectral effect is quite negligible in the present work. However, in large samples as used in some previous investigations on U^{235},[4] this could contribute, in principle at least, to the larger measured τ_1 values; i.e., the energy of the first delayed neutron group is markedly lower,[5] hence slightly more effective in producing fission, than the other groups.

Effects due to these various perturbations are, of

course, assimilated in the least-squares analysis, thus perturbing slightly the final period and abundance values. Nevertheless, since the decay of delayed neutron activity from the various fissile nuclides can be satisfactorily fitted by six periods having approximately the same values, it is reasonable to conclude that six main precursors do predominate despite evident "perturbations."

In contrast to the relative constancy of delayed neutron periods, the observed variations in both relative and total yields among the different fissile nuclides are large indeed (cf. Tables I and II). The essential problem then is to explain individual group yield values -- these being the product of relative group and total absolute yields. Calculations of precursor yields for the various fissionable nuclides have been made in terms of appropriate mass and charge distributions, including shell effects. Comparison of precursor yields thus calculated with measured delayed neutron yields for the various nuclides then gives neutron-to-β branching ratios which may be related to theoretical branching ratios. This treatment provides criteria which have proved useful in predicting the probable precursor(s) associated with a given delayed neutron group. The predictions re-

sulting from preliminary calculations have been given.[20] The results of final (machine) calculations are included in a companion paper[21] on theoretical interpretation of delayed neutron phenomena.

A useful check on the U^{235} fast-fission yield reported in Table III is provided by independent measurements of the mass increment between delayed and prompt critical for Godiva. From these measurements it has been determined that

$$\gamma_G f(U^{235}) = 0.0067 \pm 0.0002^*$$

where γ_G is the ratio of effectiveness of delayed neutrons (in producing further fissions) to effectiveness of prompt neutrons for Godiva. Taking $\gamma_G = 1.05$ and $\nu_G(U^{235}) = 2.56$, we have

$$n/F(U^{235}) = 0.0164 \pm 0.0006$$

in agreement with the corresponding value of 0.0165 ± 0.0005 from Table III.

An independent check on the U^{235} data of Table I is possible through the relation between reactor stable period and reactivity -- sometimes called "inhour equation." Of

---

*Data from H. C. Paxton, LASL.

the three units of reactivity in common use,* we use here the dollar because of its particular adaptability to the reactivity region (between delayed and prompt critical) of practical interest in fast systems. We have

$$\text{Reactivity in dollars} \equiv \frac{\Delta K}{K\gamma\beta} = \frac{\tau_p}{\gamma\beta TK} + \sum_{i=1}^{6} \frac{\gamma_i \beta_i \tau_i}{\gamma\beta (T + \tau_i)} \quad (9)$$

where

$K \equiv$ neutron reproduction number of system, $\Delta K \equiv K - 1$

$\tau_p \equiv$ prompt neutron lifetime ($\sim 10^{-8}$ sec in Godiva)

$T \equiv$ stable reactor period

$\gamma \equiv$ effectiveness (in producing fission) of delayed neutrons compared to prompt neutrons

β (also called f) $\equiv$ delayed neutron fraction of total neutrons from fission

$\tau_i \equiv$ observed mean life of i^{th} delayed neutron group

---

*The units are: (1) the "inhour" defined as the reactivity increment above delayed critical which will give T = 1 hr (this unit now generally used only for large reactors with characteristically small excess available reactivities); (2) $\Delta K/K$, a single-fiducial unit which expresses relative, or percentage, departure from delayed critical; and (3) $\Delta K/K\gamma\beta$ (the dollar), a double-fiducial unit of reactivity expressed in terms of the interval between delayed and prompt critical (γ here is an average of the six γ_i). The dollar is divided into 100 units, called cents. Thus, for a U^{235} assembly, 110¢ represents a $\Delta K/K$ of 1.10 $\gamma\beta \simeq$ (1.10 x 1.05 x 0.0165)/2.56 = 0.0074 or an effective $K \simeq 1.0074$.

In a practical calculation it is not necessary to take account of the γ_i's for individual delayed neutron groups. Instead, the measured values of relative group abundances, a_i/a, may be substituted for $\gamma_i \beta_i/\gamma\beta$ in Eq. 9 with small loss of accuracy. Equation 9 reduces to $\Delta K/K\gamma\beta \approx 1$ for Godiva at prompt critical, viz., $\tau_p \ll T \ll \tau_i$. The inhour equation becomes most sensitive to short-period delayed neutron data when T is the order of short τ_i, which occurs in the reactivity region slightly below prompt critical. Measurements of period versus reactivity have been made on the Godiva assembly; Fig. 5 compares these measurements with Eq. 9, using the data of Table I.* The experimental agreement near prompt critical provides (1) a sensitive check on accuracy of short-period delayed neutron data, and (2) good evidence against the existence of a seventh, shorter delayed neutron period of appreciable abundance (i.e., if a seventh group exists, its yield should be less than $\sim 5 \times 10^{-4}$% in U^{235} fission).

Further experimental evidence in support of short period (especially sixth-group) values is given by recent

*Similar measurements have been made on "Jezebel" (the bare Pu^{239} critical assembly at LASL) as a check on delayed neutron data for Pu^{239}. Periods between 5 and 200 sec have been measured, with good agreement. Period vs reactivity measurements will also be made on a bare U^{233} assembly soon to be installed at the LASL critical assemblies laboratory.

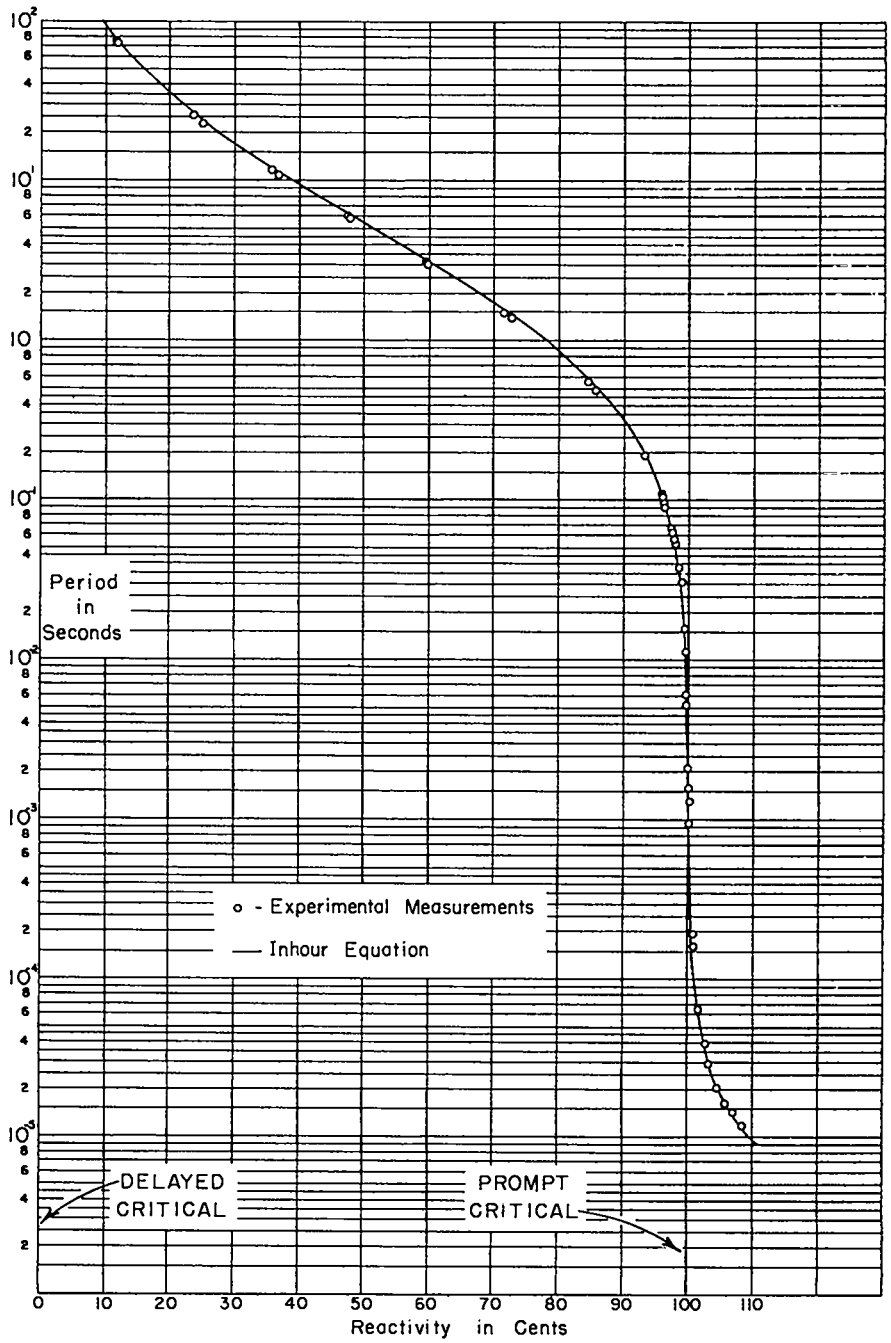

Fig. 5. Period (e-folding time) vs reactivity for the bare U^{235} assembly. The smooth curve is the Inhour Equation with data of Table I; points are measured periods (e-folding times).

studies on the detailed shape of super-prompt-critical radiation bursts (such as used in the present delayed neutron program) from the bare U^{235} assembly.[9,22] By means of a reactivity booster, the assembly can be brought suddenly to a predetermined reactivity value slightly above 100 cents. At the higher reactivities ($\sim$110¢) fission rate rises extremely rapidly to a peak power of nearly 10^4 Mw. Termination of the burst is automatic, due to the large decrease in reactivity resulting from thermal expansion. Some characteristics of a typical burst are: (1) initial rise, exponential, with T $\sim$ 15 μsec; (2) burst shape, bell-shaped near peak; (3) burst duration, $\sim$3T = "spike" width at half-maximum; (4) energy release, $\sim 10^{16}$ fissions or 0.1 KWH.

Following a burst, the fission rate drops to a residual level, "pedestal," sustained by delayed neutrons and finally terminated by automatic "scramming" (separation) of the assembly. The detailed shape of this pedestal can be calculated, in certain limiting cases, from the pile kinetic equations (space-independent, one-group model) which involve directly the periods and abundances of delayed neutrons. Calculated pedestal shape can then be compared with experimentally observed shape, thus providing a sensitive check on delayed neutron parameters (particularly short-period data). In first approximation, the pedestal shape should, of course,

exhibit the characteristic decay following an "instantaneous" irradiation (e.g., as represented by the integrand in Eq. 8). However, a more accurate prediction of burst shape must take account of the high self-multiplication of the Godiva assembly as well as rapid expansion or contraction of the U^{235} metal due to thermal heat generation or loss. It was found that initial discrepancies between theoretical and experimental burst shape could be accounted for by "room-return neutrons," i.e., by the addition of two virtual delayed neutron groups whose periods (1 - 10 msec) were the order of mean transit time for neutrons confined to the assembly room. Disappearance of the effect when bursts were repeated outdoors (assembly $\sim$10 m above ground) provided confirmation of the room-return hypothesis.

Note added in proof

Shortly after termination of the delayed neutron program, the original Godiva assembly was damaged and subsequently replaced with a similar facility, "Godiva II." This is a remote-control, bare U^{235} cylindrical assembly designed specifically as a prompt burst facility.

Appendix

SAMPLE SELF-MULTIPLICATION CORRECTION

Consider a burst irradiation producing F_o fissions and Σ_o delayed neutron precursors in a small sample just prior to t = 0. It is desired to measure the ratio Σ_o/F_o ($\equiv$ n/F). The escape probability for a delayed neutron born within the sample is $1 - (\Sigma_f + \Sigma_c)\ell_o$, where Σ_f and Σ_c are appropriately averaged macroscopic cross sections for fission and nonfission capture, respectively, and ℓ_o is the average path length of a delayed neutron within the sample. Now $\nu \Sigma_f \ell_o$ neutrons are released as a result of fission capture, and, to first order, the total number of neutrons escaping the sample per delayed neutron born is $1 + (\nu - 1 - \alpha)\Sigma_f\ell_o$, where $\alpha \equiv \Sigma_c/\Sigma_f$. This process increases the observed number of fissions in the sample by $\Sigma_f\ell_o$ per delayed neutron. Therefore, as a first order approximation, we have

$$\frac{\Sigma_{NC}}{F_s} = \frac{\Sigma_o\left[1 + (\nu - 1 - \alpha)\Sigma_f\ell_o\right]}{F_o + \Sigma_o\Sigma_f\ell_o}$$

$$\cong \frac{\Sigma_o}{F_o}\left[1 + (\nu - 1 - \alpha - \frac{\Sigma_o}{F_o})\ \Sigma_f \ell_o\right]$$

where Σ_{NC} and F_s are defined in Section IV-B as total neutron counts following an instantaneous irradiation and as total fissions, respectively. The above expression may be written as

$$n/F \equiv \frac{\Sigma_o}{F_o} \cong \frac{\Sigma_{NC}}{F_s}\left[1 - (\nu - 1 - \alpha)\Sigma_f \ell_o\right]$$

since

(1) $(\nu - 1 - \alpha)$ is the order of unity

(2) Σ_o/F_o is the order of 10^{-2}

(3) Σ_f <0.1 cm^{-1} for ordinary fissile materials

(4) ℓ_o is the order of 0.2 cm for the samples used

Thus a typical correction for a U^{235} cylindrical sample 1/8 in. in diameter and 1/2 in. long would give ℓ_o = 0.19 cm and $(\nu - 1 - \alpha)\ \Sigma_f \ell_o$ = +1.5%. The correction for similar Pu^{239} or U^{233} samples would be nearly twice that for U^{235}. Corrections for U^{238} and Th^{232} are negligible.

REFERENCES

1. R. Roberts, R. Meyer, and P. Wang, Phys. Rev., 55, 510 (1939).

2. R. Roberts, R. Meyer, L. Hafstad, and P. Wang, Phys. Rev., 55, 664 (1939).

3. N. Bohr and J. A. Wheeler, Phys. Rev., 56, 426 (1939). See also J. Frenkel, J. Phys. U.S.S.R., I, 125 (1939).

4. G. R. Keepin in Progress in Nuclear Energy, Series I, Vol. 1, p. 191 (Pergamon Press, London, 1956).

5. R. Batchelor and H. R. McK. Hyder, J. Nuclear Energy, 3, 7 (1956).

6. G. R. Keepin and T. F. Wimett, Paper 831 in Proceedings of the International Conference on the Peaceful Uses of Atomic Energy, Vol. 4, p. 162 (United Nations, New York, 1956).

7. R. E. Peterson and G. A. Newby, Nuclear Sci. and Eng., 1, 112 (1956).

8. L. Rosen, Paper 582 in Proceedings of the International Conference on the Peaceful Uses of Atomic Energy, Vol. 4, p. 97 (United Nations, New York, 1956). See also L. Cranberg, R. B. Day, L. Rosen, R. F. Taschek, and M. Walt in Progress in Nuclear Energy, Series I, Vol. 1, p. 107 (Pergamon Press, London, 1956).

9. H. C. Paxton, Nucleonics, 13, No. 10, 48 (1955).

10. P. G. Koontz, G. R. Keepin, and J. E. Ashley, Rev. Sci. Instr., 26, 352 (1955).

11. A. O. Hanson and J. McKibben, Phys. Rev., 72, 673 (1947).

12. P. G. Koontz, C. W. Johnstone, G. R. Keepin, and J. D. Gallagher, Rev. Sci. Instr., 26, 546 (1955).

13. W. E. Deming, Statistical Adjustment of Data (John Wiley

and Sons, New York, 1943).

14. G. A. Jarvis, C. I. Browne, and G. W. Knobeloch, LASL, private communication.

15. J. A. Harvey and J. E. Sanders in Progress in Nuclear Energy, Series I, Vol. 1, p. 1 (Pergamon Press, London, 1956).

16. J. E. Terrell (to be published).

17. R. B. Leachman, Phys. Rev., 101, 1005 (1956).

18. D. J. Hughes, J. Dabbs, A. Cahn, and D. B. Hall, Phys. Rev., 73, 111 (1948).

19. L. E. Glendenin and E. P. Steinberg, Paper 614 in Proceedings of the International Conference on the Peaceful Uses of Atomic Energy, Vol. 7, p. 3 (United Nations, New York, 1956). See also L. E. Glendenin, Report NP-1242 (MIT Laboratory for Nuclear Science Technical Report 35), December 1949.

20. G. R. Keepin, Phys. Rev., 106 (June 15, 1957).

21. G. R. Keepin, "Interpretation of Delayed Neutron Phenomena," Los Alamos Scientific Laboratory Report, in preparation.

22. T. F. Wimett, G. A. Graves, and J. D. Orndoff, Nuclear Sci. and Eng. (to be published, 1957). See also Los Alamos Scientific Laboratory Report LA-2029, April 1956.